ACS OMEGA

http://pubs.acs.org/journal/acsodf

Article

Effects of Acoustic Excitation on the Combustion Instability of Hydrogen−Methane Lean Premixed Swirling Flames

Kai Deng,* Yi Zhong, Mingxiao Wang, Yingjie Zhong, and Kai Hong Luo

Cite This: https://dx.doi.org/10.1021/acsomega.0c00287

Read Online

ACCESS | Metrics & More | Article Recommendations

ABSTRACT: Lean premixed flames are useful for low nitrogen oxide (NO_x) emissions but more prone to induce combustion instability in gas turbines. Combustion instability of a lean premixed swirling flame (LPSF) with hydrogen−methane was investigated experimentally. The effects of hydrogen addition on combustion instability with equivalence ratios 0.75−1 were investigated with acoustic frequencies (90−240 Hz) and acoustic amplitudes (the ratio of velocity fluctuation to an average velocity of 0−0.5), respectively, which are characterized by the gain and phase of the flame describing function (FDF). The evolution of vortex and the flame morphologies were observed by the particle image velocimetry (PIV), intensified charge-coupled device (ICCD), photomultiplier tube (PMT), and Cassegrain optical systems. The global and local heat release fluctuations of the LPSF were shown by CH*/OH* chemiluminescence and temperature measurements. Results show that the FDF features maximum and minimum gain values in the acoustic frequency range of 90−240 Hz and reaches local maximum peaks at 110 and 180 Hz and local minimum peaks at 160 Hz. It can also be observed that varying velocity amplitudes (0−0.5) have greater effects on the gain and phase of FDF than changing equivalence ratios (0.75−1) for lean swirling flames. Higher velocity amplitudes more effectively intensified the compression of the flame length, which enhanced the mixing of the high-burning gas and the unburned gas, and then heat release fluctuations increased. However, it is more interesting that the effects of hydrogen addition on the combustion instability of the LPSF show a completely opposite phenomenon due to acoustic frequency under all experimental conditions. The FDFs were compared at typical frequencies of 140 and 180 Hz, and it was found that combustion instability enhanced with increasing hydrogen content at 140 Hz while weakened at 180 Hz. The flow field of PIV images shows that it is related to the location and development of vortices in the flame with varying acoustic frequencies. The intensity of OH*/CH* chemiluminescence, local temperature, and heat release rate show the same changing trend with the flame morphology for two acoustic parameters with the increasing hydrogen content in the LPSF. This directly affects the compression and curvature of the LPSF and thereby changes the mixture and temperature of the combustible gas, which influence the heat release fluctuation of the LPSF.

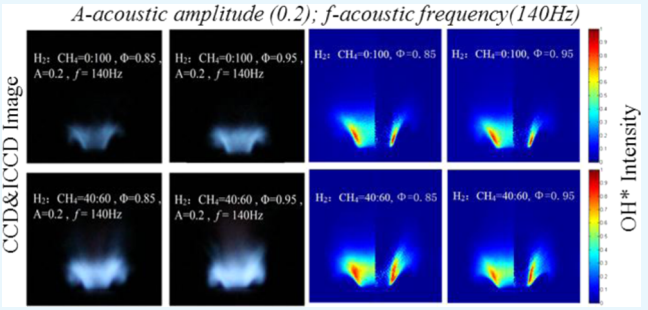

1. INTRODUCTION

Lean premixed flames are useful for low nitrogen oxide (NO_x) emissions but more prone to induce combustion instability in gas turbines,[1] which is also known as thermoacoustic instability typically generated by the interaction between unsteady heat release oscillation and pressure fluctuation. The instability grows due to the acoustic energy supplied by the flame, so combustion instability is determined by the flame response.[2] This unstable combustion phenomenon can damage the structure of the device,[3−6] which is an important technical problem worldwide. Researchers investigated the mechanism of combustion instability including flame surface fluctuation,[7,8] equivalence ratio fluctuation,[9,10] entropy wave fluctuation,[11] and vortex shedding[12] and found that heat release oscillation changing with the flame response to flow field is the fundamental basis of the combustion instability; therefore, the most important factor is to understand how the changes in heat release fluctuation are caused by the flame response to acoustic excitation.[7−12]

Recently, with the increasing application of synthetic natural gas, more research studies on H_2/CH_4 have been reported. Compared with traditional fuels, syngas fuels show definitely different combustion characteristics. Experimental results with simplified burners have shown that the addition of hydrogen to methane could improve energy density,[13] increase laminar burning velocity,[14] extend flashback limit, change ignition

Received: January 22, 2020
Accepted: March 27, 2020

characteristics,[15,16] enhance flame stability, and reduce NO_x emission.[17,18]

The addition of hydrogen to fuel influences both the chemical and physical processes in the flame. Researchers have proposed different opinions on the effects of hydrogen addition on flame instability. Di Sarli[19] investigated the effects of hydrogen content on lean premixed flame dynamics and observed that the higher hydrogen content influences the flame burning rate and flame surface area, then generates the pocket phenomenon and affects the flow field quantitatively and qualitatively. Schefer[20] found that the higher OH concentration with the addition of up to 20% hydrogen content occurs near the outer shear layer of the lean premixed swirling flame, thereby extending the lean stability limits of the burner. Yilmaz's[21] research studies show that hydrogen addition results in a significant change in the combustion characteristics of the mixture and increases flame compression at ranges of acoustic frequencies. The thermoacoustic coupling phenomenon and acoustic response at the base of the flame show different characteristics with resonant and nonresonant frequencies. Kim[22] proposed that the higher diffusivity of hydrogen content accelerates the premixing velocity, resulting in a decrease in the elapsed time of the high-temperature reaction zone. García-Armingol[23] investigated the relationship between flashback and combustion instabilities of hydrogen-enriched fuels and found that hydrogen addition is prone to induce periodic tempering, leading to changes in flame fronts and temperature fluctuations, which in turn lead to higher velocity fluctuations and thermoacoustic oscillations. However, other researchers observed that hydrogen addition inhibits combustion instability. Taamallah[24] observed that hydrogen addition causes the value of the strain rate function to become smaller and decreases combustion instability, which appears in the external recirculation zone. Barbosa[25] concluded that hydrogen addition significantly causes increasing flame length, decreasing flame width and heat release, and declining combustion instability. Emadi[26,27] found that the degree of thermoacoustic oscillation at the root position of the mixed gas flame with 40% of hydrogen content at 135 Hz acoustic frequency of sound is significantly reduced. Therefore, the addition of hydrogen is considered to be an effective method to suppress combustion instability.

Due to the higher reactivity of hydrogen fuel, the effects of hydrogen addition on flame for improving flashback and ignition could be well understood. However, the practical applications of hydrogen−methane are still limited due to the lack of laws and mechanisms of the interaction between hydrogen and methane and complicated flow field. A full investigation of the effects of hydrogen content on flame with acoustic parameters will be not only beneficial for controlling the phenomenon of combustion instability but also helpful for understanding flame propagation in industrial burners with hydrogen-rich fuels. In conclusion, the response of flame dynamics to acoustic excitation due to hydrogen fraction deserves more in-depth research.

Our group has obtained the combustion instability characteristics of methane/hydrogen lean premixed swirl flames.[28] Now we conduct further research on the effects of hydrogen addition on the combustion instability of the hydrogen−methane lean premixed swirling flame (LPSF) by examining the flame response to a range of equivalence ratios, acoustic frequencies, and velocity amplitudes induced by acoustic excitation. Four different blends of hydrogen and methane were applied as fuels at equivalence ratios of 0.75−1, with acoustic frequencies of 90−240 Hz and acoustic amplitudes (the ratio of velocity fluctuation to an average velocity of 0−0.5. The flame describing functions (FDFs) are used to describe the effects of hydrogen content on the combustion instability of swirling flame at different acoustic parameters. The effects of hydrogen content on combustion instability were analyzed by the dynamic response of the LPSF to acoustic excitation, including FDF, vortex evolution shown by particle image velocimetry (PIV) images, the flame structure shown by OH* and CH*, local temperature, and heat release rate of the flame.

2. EXPERIMENTAL SYSTEM

2.1. Experimental Apparatus. To investigate the effects of hydrogen addition on thermoacoustic instability, it is necessary to establish a relatively independent combustor and adjustable acoustic devices for measuring the flame response to acoustic forcing. The experimental apparatus is shown in Figure 1. It is an

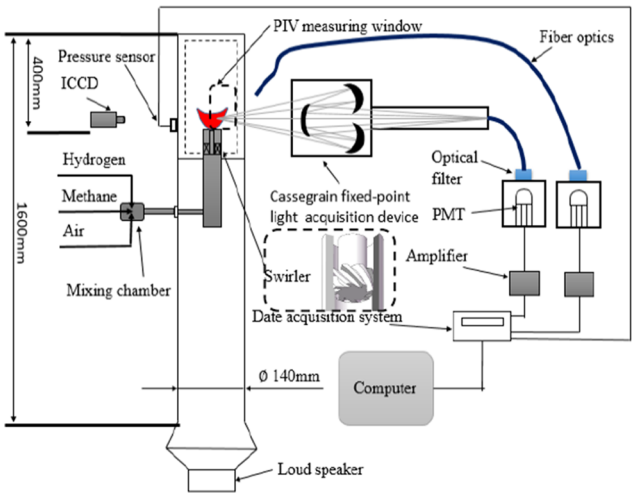

Figure 1. Experimental system.

annular tube with a diameter of 140 mm and height of 1600 mm, which consists of two parts, the upper part is an optically accessible quartz combustion chamber with a swirl combustor and the lower part is a loudspeaker. Combustion instability in engineering applications is related to low-frequency and high-amplitude thermoacoustic oscillations. The loudspeaker that is placed at the bottom of the tube can generate a forced acoustic wave. The acoustic signal is amplified by the power amplifier to form an adjustable acoustic amplitude and frequency.

Experiments were performed in a swirl combustor of hydrogen−methane fuel, with a swirl number of 0.8 and vane angle of 43.5°, which is commonly used in gas turbines. The swirl combustor consists of eight swirl blades with an outer diameter of 12 mm and inner diameter of 8 mm. Methane, hydrogen, and air are controlled by the thermal mass flow controllers (SHENGYE, SY-93) with a measuring accuracy of 1.5% full range. The mixture of fuel and air is injected into a mixing chamber, which is connected to the swirl combustor. The flame excited by the loudspeaker could be observed and recorded through the quartz windows with a length of 90 mm and height of 400 mm.

The dynamic response of the LPSF to acoustic excitation is analyzed by heat release oscillation, flame morphology, temperature distribution, and CH*/OH* chemiluminescence. The flame front and the flow field are recorded by experimental instruments, including the photomultiplier tube (PMT,

https://dx.doi.org/10.1021/acsomega.0c00287
ACS Omega XXXX, XXX, XXX−XXX

Hamamatsu R928), intensified charge-coupled device (ICCD) camera (Andor DH334), micro-thermocouple, particle image velocimetry (PIV) system, and Cassgrain optical system.

The most important parameters to illustrate the flame dynamic response are the value of heat release oscillation and flame images. Research studies have shown that the whole heat release rate for the lean premixed flame is proportional to the intensity of OH* chemiluminescence.[29,30] Thus, OH* chemiluminescence emissions obtained by a photomultiplier tube (PMT, Hamamatsu R928) with the OH filter (315 ± 10 nm) are used for illustrating the intensity of the heat release rate in the chemical reaction zone for the positive relationship between them. The local heat release fluctuation of the flame was obtained with a diameter of 0.382 mm in the flame by a series of reflections, which is called the Cassegrain system.[31] This noncontact system was designed using the Cassegrain optical principle to detect dynamic chemiluminescence signals on a point inside the flame.

The instantaneous flame images could reflect flame morphology especially the flame front structure, which could be assessed by CH* chemiluminescence. The whole flame front structures were obtained by an ICCD camera (Andor DH334) with a CH* chemiluminescence filter (427 ± 10 nm), and a two-dimensional (2D) flame section was shown by the Abel deconvolution scheme.[32,33]

The phase-locked images of the flow field were obtained by the PIV system including a YAG laser (double 150 mJ pulses at 532 nm) and 4M digital camera (2048 × 2048 pixels) with 3 μm Al_2O_3 particles mixed with the fuel. Due to the symmetry of the flame, the PIV system records the right side of the flame (40 mm × 50 mm) to show vortex development, and images are analyzed by the 2D cross-correlation fast Fourier transform (FFT) algorithm. PIV images and the acoustic field are triggered simultaneously and recorded by the phase-locked measurement to obtain a transient flame structure.

To accurately measure the acoustic velocity amplitude at the location of the flame, the P−P method with two microphones was used. The principle of the P−P method to measure acoustic velocity fluctuation is shown in Figure 2.[28] NI-DAQ acquisition was used for obtaining the data of velocity fluctuation and heat release fluctuation synchronously.

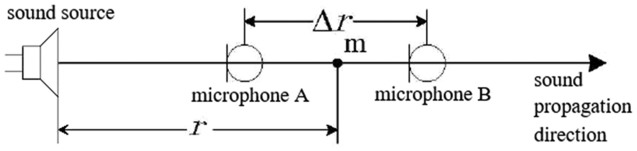

Figure 2. Schematic of the P−P method.

In Figure 2, m is the midpoint of microphones A and B, r is the distance between the sound source and m, and Δr is the distance between microphones A and B. According to the one-dimensional Euler equation, the velocity of location m can be expressed as

$$u(t) = -\frac{1}{\rho_0}\int \frac{\partial p(t)}{\partial r}\,\mathrm{d}t \tag{1}$$

where $u(t)$ is the acoustic velocity, ρ_0 is the density of the acoustic medium, and $\frac{\partial p(t)}{\partial r}$ is the sound pressure gradient in the sound propagation direction, which can be approximated by the first-order finite difference when the distance between the two microphones is far less than sound wavelength $\Delta r \ll \lambda$, that is

$$\frac{\partial p(t)}{\partial r} = \frac{p_B(t) - p_A(t)}{\Delta r} \tag{2}$$

Substituting eq 2 into eq 1, we can get the acoustic velocity as

$$u(t) = -\frac{1}{\rho_0}\int \frac{p_B(t) - p_A(t)}{\Delta r}\,\mathrm{d}t \tag{3}$$

2.2. Experimental Conditions. The experimental parameters including hydrogen contents, equivalence ratios, acoustic frequencies, and acoustic amplitudes are shown in Table 1. Research results show that the addition of 20% hydrogen to fuel leads to a transition from a wrinkled regime to a more vigorous regime,[21] a significant increase in OH concentration, and extension of the lean limit,[22] sufficiently inducing flame-acoustic close coupling.[23] Therefore, experiments were run for the lean mixture with the four blends of hydrogen contents (0, 10, 20, 40%).

Equivalence ratio fluctuation is also one of the important parameters for combustion instability due to its strong effects on heat release fluctuation, which has been proposed as one of the four basic mechanisms,[7−12] besides flame surface fluctuation, entropy wave fluctuation, and vortex shedding. Therefore, the equivalence ratios of 0.75−1 for the LPSF were selected for comparative investigation; due to this, ranges of equivalence ratios are also used in gas turbines to meet low NO_x emission requirements.

Research studies show that when combustion instability occurs, the flame usually acts as an amplifier in the lower frequency range and its response depends on the acoustic amplitude.[34] Also, the visible flame structure significantly changes with the acoustic frequency varying from 100 to 220 Hz.[27] Thus, experimental conditions including acoustic velocity amplitudes of 0−0.5 and acoustic frequencies from 90 to 240 Hz were used and adjusted by the loudspeaker (JBL A0208A) with the acoustic wave generator (GWINSTEK AFG-2225).

The equivalence ratio φ is calculated according to eq 4,[35] where α is the mole fraction of hydrogen in the mixture, m is the mass of gas, and MW is the molar mass of gas.

Table 1. Experimental Parameters

operating condition	hydrogen flow rate (N mL/min)	methane flow rate (N mL/min)	equivalence ratio (φ)	acoustic frequency (f) (Hz)	acoustic amplitude (ratio of velocity fluctuation to average velocity) (A)
1	0	1000	0.75−1.0	90−240	0−0.5
2	100	900			
3	200	800			
4	400	600			

https://dx.doi.org/10.1021/acsomega.0c00287
ACS Omega XXXX, XXX, XXX−XXX

$$\varphi = \frac{\frac{m_{fuel}}{m_{air}}}{(m_{fuel}/m_{air})_{stoich}} = \left(\frac{m_{fuel}}{m_{air}}\right) \times \frac{\left(2 - \frac{3\alpha}{2}\right) \times (MW_{O_2} + 4MW_{N_2})}{(1-\alpha)MW_{CH_4} + \alpha MW_{H_2}} \quad (4)$$

The equivalence ratios are achieved by adjusting the corresponding air volume with constant fuel volume as hydrogen contents varied, which are effective as experimental ranges of hydrogen contents.[23] These can be precisely controlled within a measuring accuracy of 1.5% full range. The laminar combustion conditions are conducted so that the impact of the acoustic excitation can be shown more clearly. Each group of experimental conditions was operated three times, and the average results were taken. The uncertainty of the results could be controlled within 1.5%.

2.3. Flame Describing Functions. The FDF, which is a function of acoustic frequencies and amplitudes, represents the dynamic response of the heat release oscillation by incoming velocity perturbations.[36−39] The relationship between the velocity perturbations and heat release oscillations could be constructed by the FDF. The FDF is defined as follows

$$F(f, u') = \frac{Q'/\bar{Q}}{u'/\bar{u}} \simeq \frac{I'_{OH*}/\bar{I}_{OH*}}{u'/\bar{u}} \quad (5)$$

where $\bar{Q}$ is the whole time-averaged heat release rate, $\bar{u}$ is the injector bulk velocity, and Q' and u' are the corresponding fluctuations of the whole heat release rate and bulk velocity under an acoustic frequency, respectively. A represents a dimensionless acoustic velocity amplitude, which is defined as the ratio of velocity fluctuation to the injector bulk velocity. The heat release rate is obtained by measuring the total light emissions of excited radicals OH* with a photomultiplier. The FDF can be expressed as

$$F(f, A) = H(f, u')\, e^{i\Phi(f,u')}, \quad A = \frac{u'}{\bar{u}} \quad (6)$$

where H reflects the gain of the FDF and the phase Φ defines the time delay between the velocity fluctuation and the heat release rate. The higher gain of the FDF means greater effects of velocity fluctuation on heat release fluctuation and stronger combustion instability.

3. RESULTS

First, the laws of the FDF gain with ranges of acoustic frequencies (90−240 Hz) at various hydrogen contents (0, 10, 20, 40%) were investigated experimentally. Then, the FDFs of the LPSF varying with equivalence ratios of 0.75−1 under the acoustic frequency of 140/180 Hz were compared. Finally, the results of the FDF changing with acoustic velocity amplitudes of 0−0.5 under the acoustic frequency of 140/180 Hz with the increasing hydrogen content were reported.

3.1. Effects of Hydrogen Contents on the FDF of Swirling Flame Varying with Acoustic Frequencies. Experiments were conducted to investigate the variation of the FDF gain with the acoustic frequency at various hydrogen contents. The results are shown in Figure 3 at the acoustic velocity fluctuation of 0.3 and an equivalence ratio of 0.8. The following features can be observed:

(1) It is interesting to show that the FDF features maximum and minimum gain values in the low-frequency range (90−240 Hz). For a given hydrogen content, the FDF gain fluctuated significantly following an increase in acoustic frequency and reached local maximum peaks at 110 and 180 Hz and local minimum peaks at 160 Hz. The repeated increase and decrease in the FDF gain were observed with varying acoustic frequencies.

(2) When the acoustic frequency increased from 90 to 110 Hz or from 160 to 240 Hz, the FDF gain decreased following an increase in the hydrogen content, which indicates that the flame response was less sensitive to disturbances, and the effects of acoustic excitation on heat release fluctuation became weaker. It is beneficial for controlling combustion instability. On the contrary, the FDF gain increased with an increase in the hydrogen content within the range of 110−160 Hz, which implies that the combustion instability of the LPSF can be more easily induced.

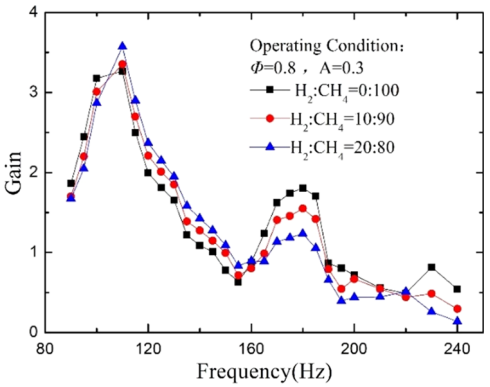

Figure 3. Variation of the FDF gain with acoustic frequency.

3.2. Effects of Hydrogen Contents on the FDF of Swirling Flame Varying with Equivalence Ratios. In this section, the flame describing functions with ranges of hydrogen contents at an equivalence ratio range of 0.75−1 were obtained. The structures of the flame front, vortices in the flame flow field, OH* chemiluminescence intensity, local temperature, and heat release fluctuation were also obtained to show the law of combustion instability.

Figure 4 shows the effects of the hydrogen content on the flame transfer function with the equivalence ratio range of 0.75−1 and the acoustic velocity fluctuation of 0.2 at an acoustic frequency of 140/180 Hz. The gain of the FDF slightly increased with the equivalence ratio and reached a plateau, and then decreased as the equivalence ratio increased. At an equivalence ratio of 0.75−1, the gain of the FDF ($|H|$) increased with the hydrogen content at the acoustic frequency of 140 Hz but decreased at 180 Hz. The higher gain of the FDF showed that the effects of velocity fluctuation on combustion instability are stronger. The opposite phenomenon was observed at 180 Hz. The combustion instability was enhanced with the high hydrogen content at 140 Hz and decreased at 180 Hz at equivalence ratios of 0.75−1.

The phase of the FDF (Figure 4) indicates that the higher hydrogen contents cause an increase in the phase of the FDF and it moves away from 2π at both acoustic frequencies of 140 and 180 Hz. The phase signal can show a global delay of dynamical interaction between the modulation of the incoming velocity and heat release fluctuations. The phase difference between the heat release oscillation and the velocity oscillation increased with the higher hydrogen content but still limited to 2.5π. Under

https://dx.doi.org/10.1021/acsomega.0c00287
ACS Omega XXXX, XXX, XXX−XXX

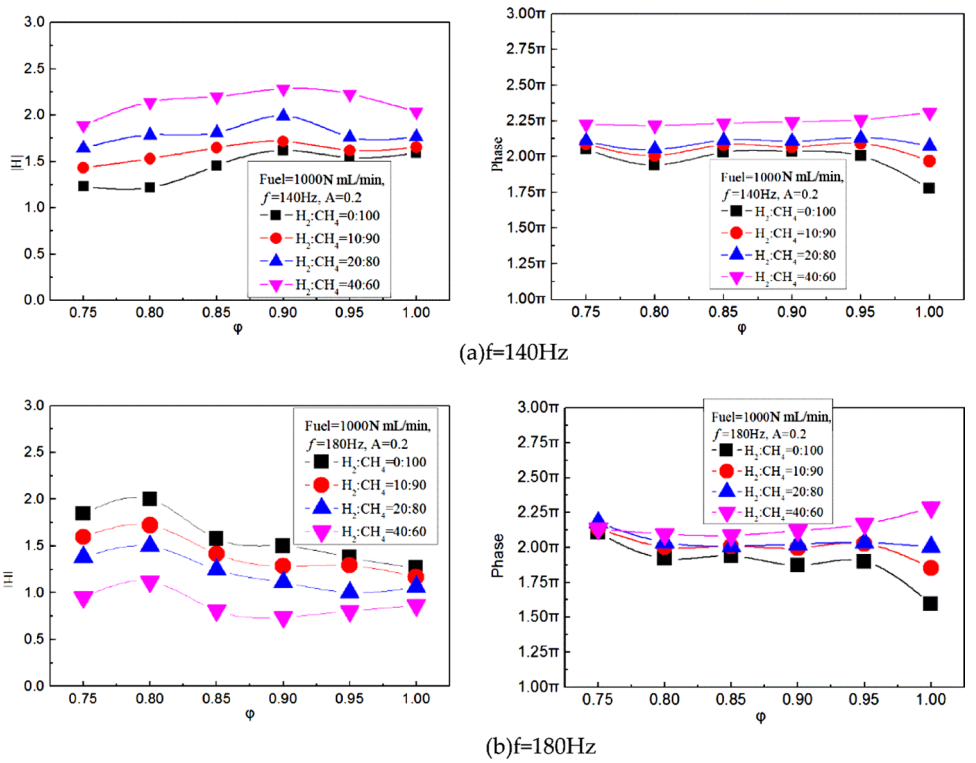

Figure 4. Effects of the hydrogen content on the flame describing function with an equivalence ratio range of 0.75−1.

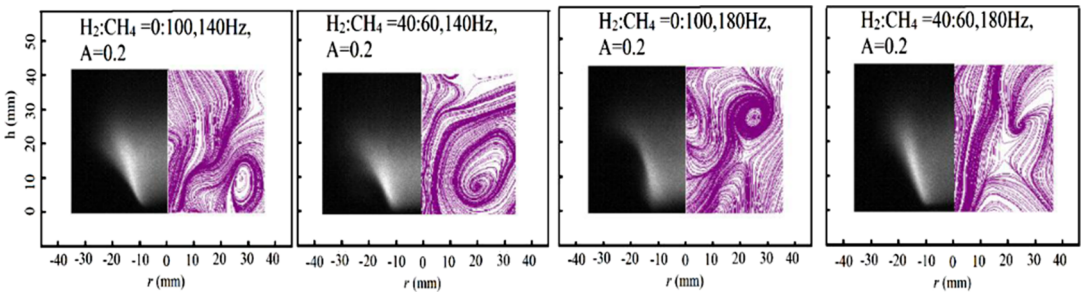

Figure 5. Effect of hydrogen content on CH* distribution (left) and flow field (right) at an equivalence ratio of 0.8.

these cases, swirling flames were still in an unstable state of combustion instability with these phase differences and did not enter another stable dynamic mode.[31] The higher hydrogen contents increased the time delay between the incoming velocity modulation and heat release rate, resulting in perturbation. We noted a phenomenon that the gain of the FDF has different trends changing with hydrogen contents, which is related to vorticity wave that has been reported by experimental studies[37,39] and simulation modeling.[40,41]

Figure 5 shows the CH* distribution and flow field of flames recorded by ICCD and PIV separately. The CH* fluorescence images (left side in Figure 5) are cumulative images in one cycle, which can show the whole flame structure and the location of flame front. The instantaneous images (right side in Figure 5) are recorded at the phase (180°) by PIV to show the vortex structure at 140/180 Hz. From CH* fluorescence images, the wider and more curved flame could be observed with higher hydrogen contents at f = 140 Hz, while the narrower flame at the upstream and a sharp curvature at the downstream region were exhibited with lower hydrogen contents at 180 Hz.

In PIV images, the larger vortex sizes at the base of the flame were shown with a higher hydrogen content under an acoustic frequency of 140 Hz, which would induce a stronger entrainment effect and mixing on the flow field of the flame, augmenting the heat release and aggravating the combustion instability.[21,26,39] The intensity of OH*, the local temperature, and local heat release fluctuation will confirm that phenomenon.

Under an acoustic frequency of 180 Hz, vortex was greatly affected by acoustic excitation at the downstream zone of the LPSF; as the hydrogen content increased, the size of the vortex became smaller, thereby decreasing the heat release fluctuations and inhibiting combustion instability. The coupling position of the flame and the vortex under acoustic excitation is very important for the whole heat release rate because the upper and lower parts of the LPSF have different phases of heat release fluctuations.[32,42]

To investigate different mechanisms of the effects of hydrogen contents on the FDF at 140/180 Hz, the local temperature and local FDF were further observed and analyzed with an equivalence ratio of 0.8.

The OH* chemiluminescence of flame front (left side) and OH* chemiluminescence distribution of the flame through Abel transformation (right side) are shown in Figure 6. There are different trends at 140 and 180 Hz with the increasing hydrogen

https://dx.doi.org/10.1021/acsomega.0c00287
ACS Omega XXXX, XXX, XXX−XXX

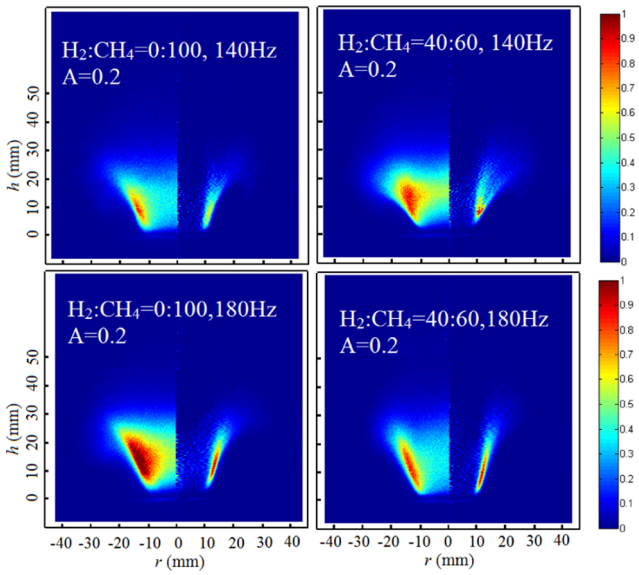

Figure 6. OH* chemiluminescence with hydrogen contents at an equivalence ratio of 0.8.

content. A longitudinal shortening flame and lateral widening flame changed with the increasing hydrogen content at 140 Hz, while the opposite phenomenon was observed at 180 Hz. Meanwhile, it was also observed that as the hydrogen content increased, the OH* chemiluminescence intensity was higher at 140 Hz and the OH* chemiluminescence intensity was lower at 180 Hz.

The downstream area of the flame decreased from the perspective of the internal circulation zone at 180 Hz, and then, the internal recirculation area of the swirling flame became smaller. This is related to the decrease in the high-temperature combustion products at the counter current returning to the bluff body of the swirler, the lower initial temperature of the premixed gas, and the decreasing chemical reaction rate.[43]

The effects of hydrogen content on the flame combustion instability at 140/180 Hz were shown by local temperature and heat release fluctuation at the position of vortex. The local OH* chemiluminescence concentration was obtained by the Cassegrain system. The local temperature was acquired by the S-type thermocouple and obtained by an average of 5000 data.

Figures 7 and 8 present the local temperature and local heat release fluctuation distribution of the LPSF under different

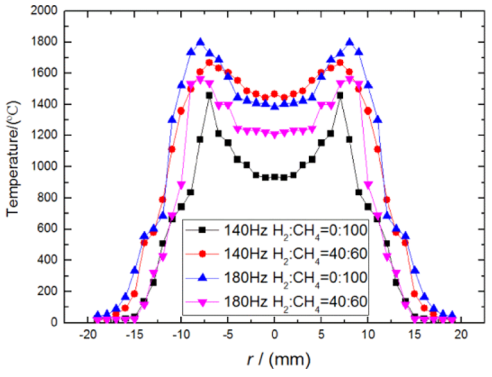

Figure 7. Local temperature distribution at the location of vortex with an equivalence ratio of 0.8.

ranges of hydrogen contents at the same position at frequencies of 140 and 180 Hz, which correspond to the location of vortex.

The gain of the local temperature and local heat release fluctuation of the LPSF increased at 140 Hz and decreased at 180 Hz with the increasing hydrogen content. Moreover, the peak area of the local temperature and local heat release fluctuation gradually widened at 140 Hz and narrowed at 180 Hz with the increasing hydrogen content. In conclusion, the increasing hydrogen content at 140 Hz expanded the flame forward and strengthened the curve of the flame surface, but it became more stable at 180 Hz. These data at the position of vortex showed that an increase of hydrogen content has opposite effects on flame instability at 140/180 Hz with equivalence ratios of 0.75−1.

In summary, with the combustion instability of the lean swirling premix flame under equivalence ratios of 0.75−1 and the increased hydrogen content, it could be concluded that the gain of the FDF slightly increased with the equivalence ratio and reached a plateau and then decreased as the equivalence ratio increased. The gain of the FDF increased at f = 140 Hz but decreased at f = 180 Hz; the phase of the FDF increased and moved away from 2π but was still in the combustion instability state in all cases. The more curving of the LPSF with higher hydrogen content was observed at f = 140 Hz but less curving at f = 180 Hz. It is related to the fact that the vortices induced by acoustic excitation have been produced in different parts of the flame at 140 and 180 Hz. The base of the LSPF was mainly influenced by the vortex for the 140 Hz case, but the downstream zone of the LSPF was affected by the vortex for the 180 Hz case. While the hydrogen content increased, a stronger or weaker entrainment effect was induced at 140 and 180 Hz, which in turn influenced the heat release oscillation, eventually influencing the combustion instability of the LSPF. The comparative results of local temperature and local heat release fluctuation have verified the conclusion.

3.3. Effects of Hydrogen Contents on the FDF of Swirling Flame Varying with Acoustic Velocity Amplitudes. The laws of combustion instability under the velocity amplitudes of 0−0.5 with increased hydrogen content are shown in Figure 9. With an increase of velocity disturbance, the gain of FDF decreased in nearly all cases, indicating that the combustion system became less susceptible to velocity fluctuations when oscillation continued to increase. Also, the phase of the FDF changed slightly with velocity amplitudes. Moreover, the increase of hydrogen content caused the gain of the FDF to become larger at 140 Hz and smaller at 180 Hz. The phase difference between the velocity oscillation and heat release fluctuation increased with an increase in the higher hydrogen content in both cases. The higher heat release oscillation could be observed with larger velocity amplitudes as shown in Figure 10. It could also be concluded from Figure 10 that as the hydrogen content increased, the heat release oscillation increased at 140 Hz and decreased at 180 Hz.

Figure 11 shows the evolution diagram of the flame front structure by CH* and OH* with different hydrogen contents under velocity amplitudes from 0 to 0.45. The increasing hydrogen content caused more curving of the flame at f = 140 Hz, while it is exactly the opposite at f = 180 Hz. It could also be observed that the higher velocity disturbance more effectively intensified the compression of the flame length, which enhanced the mixing of the high-burning gas and the unburned gas.

https://dx.doi.org/10.1021/acsomega.0c00287
ACS Omega XXXX, XXX, XXX−XXX

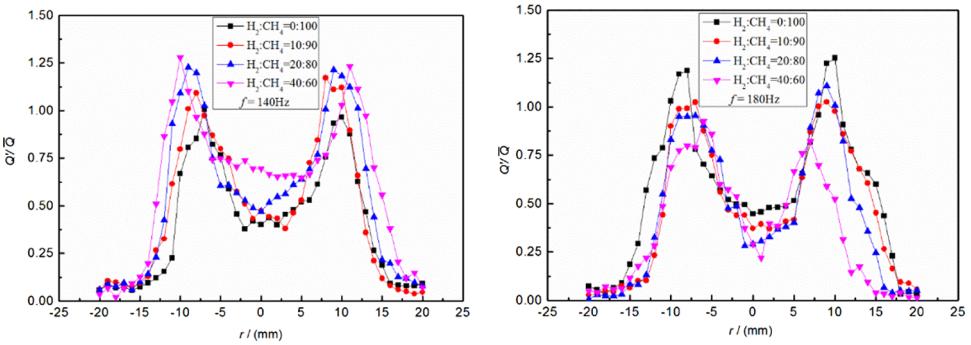

Figure 8. Local heat release fluctuation at the location of vortex with an equivalence ratio of 0.8.

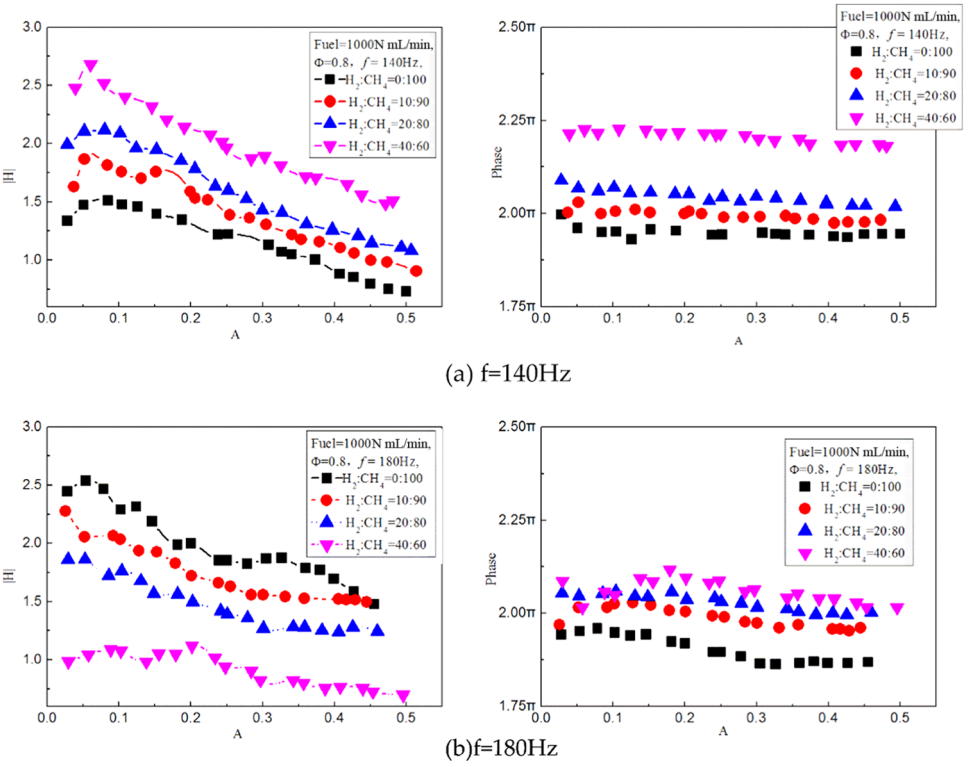

Figure 9. Influence of hydrogen contents on the flame describing function with the velocity disturbance of 0−0.5.

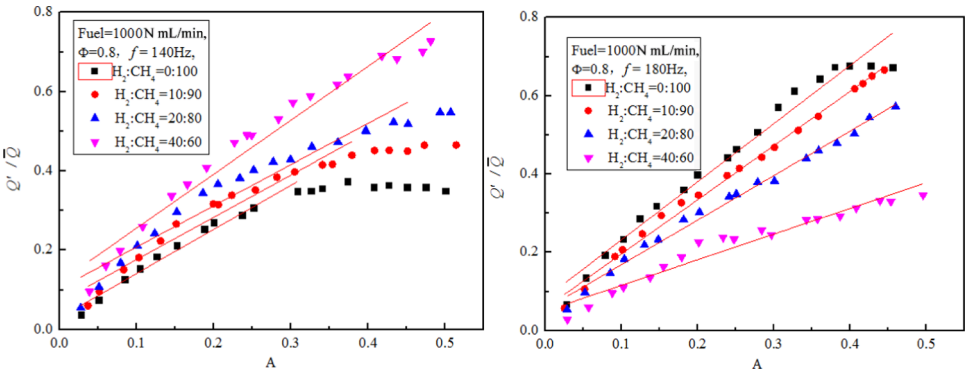

Figure 10. Effects of hydrogen contents on the heat release rate with velocity amplitudes of 0−0.5.

4. CONCLUSIONS

In conclusion, the effects of hydrogen contents on the combustion instability of the LSPF were investigated experimentally by means of determining the FDF with equivalence ratios, acoustic frequencies, and amplitudes of velocity. The effect of hydrogen contents on the combustion instability of the LSPF in response to different acoustic parameters was analyzed in terms of the flame front structure, the strength of OH* chemiluminescence, local temperature, and local heat release

https://dx.doi.org/10.1021/acsomega.0c00287
ACS Omega XXXX, XXX, XXX−XXX

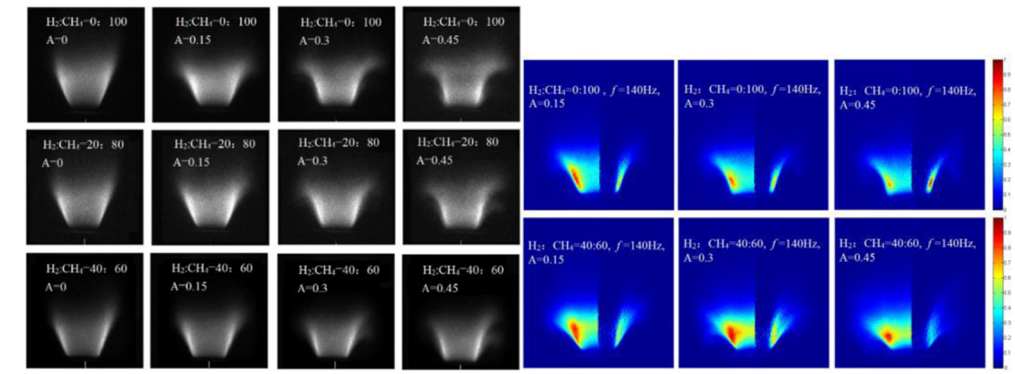

(a)f=140Hz

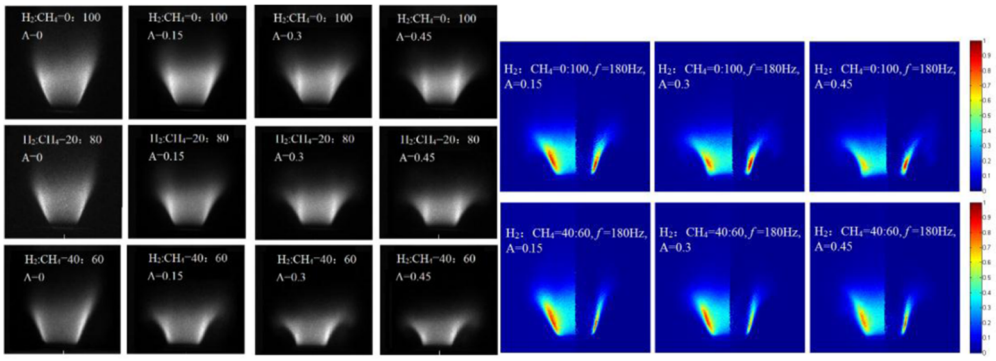

(b)f=180Hz

Figure 11. Flame front structure shown by CH* (left) and OH* (right) with different hydrogen contents under velocity disturbances from 0 to 0.45.

fluctuation by the PIV, ICCD, PMT, and Cassegrain optical systems. The results showed that

(1) FDF featured maximum and minimum gain values in the acoustic frequency range of 90−240 Hz and reached local maximum peaks at 110 and 180 Hz and local minimum peaks at 160 Hz.

(2) Over the equivalence ratio of 0.75−1, the amplitude of the FDF increased at f = 140 Hz but decreased at f = 180 Hz, while the hydrogen content increased. Concurrently, the phase of the FDF increased and moved away from 2π in all of the cases. It is related to the different vortices induced by acoustic excitation in different parts of the flame at 140 and 180 Hz. The base of the LSPF was mainly influenced by the vortex for the 140 Hz case, but the downstream zone of the LSPF was affected by the vortex for the 180 Hz case. As the hydrogen content increased, a stronger or weaker entrainment effect was induced at 140 and 180 Hz, respectively, which in turn caused the heat release oscillation to finally increase or decrease flame instability.

(3) For velocity amplitudes of 0−0.5, the gain of the FDF decreased with increasing velocity disturbances but the heat release fluctuations increased with velocity disturbances. The increase in the hydrogen content caused more curving of the flame at f = 140 Hz, while it is exactly the opposite at f = 180 Hz. It could also be observed that the higher velocity disturbance more effectively intensified the compression of the flame length, which enhanced the mixing of the high-burning gas and the unburned gas.

AUTHOR INFORMATION

Corresponding Author

Kai Deng − *Institute of Energy and Power Engineering, Zhejiang University of Technology, Hangzhou 310014, China; Department of Mechanical Engineering, University College London, London WC1E 7JE, U.K.;* orcid.org/0000-0003-0233-3442; Phone: +86-13675893253; Email: dkai@zjut.edu.cn

Authors

Yi Zhong − *Institute of Energy and Power Engineering, Zhejiang University of Technology, Hangzhou 310014, China*

Mingxiao Wang − *Zhejiang Important Laboratory of Energy Storage and Building Energy Saving Technology, Huadian Electric Power Research Institute Co., Ltd., Hangzhou 310000, China*

Yingjie Zhong − *Institute of Energy and Power Engineering, Zhejiang University of Technology, Hangzhou 310014, China*

Kai Hong Luo − *Department of Mechanical Engineering, University College London, London WC1E 7JE, U.K.;* orcid.org/0000-0003-4023-7259

Complete contact information is available at: https://pubs.acs.org/10.1021/acsomega.0c00287

Author Contributions

Conceptualization, K.D.; methodology, K.D. and M.W.; software, K.D. and Y.Z.; validation, Y.Z.; formal analysis, K.D.; investigation, K.D. and M.W.; resources, Y.Z. and M.W.; data curation, M.W.; writing—original draft preparation, K.D. and Y.Z.; writing—review and editing, K.D.; visualization, M.W.;

https://dx.doi.org/10.1021/acsomega.0c00287
ACS Omega XXXX, XXX, XXX−XXX

supervision, K.H.L.; project administration, Y.J.Z.; funding acquisition, K.D.

Funding

This research was supported by Zhejiang Provincial Natural Science Foundation of China under Grant no. LY18E060012, National Natural Science Foundation of China under Grant no. 51106139, and the China Scholarship Council under Grant no. 201708330386. K.D. received these fundings.

Notes

The authors declare no competing financial interest.

■ ACKNOWLEDGMENTS

The authors would like to thank the reviewers and editor for manuscript improvements.

■ REFERENCES

(1) Li, X. Y.; Zhao, D.; Li, S. H.; Ji, C. Z. Effect of heat source on transient energy growth analysis of a thermoacoustic system. *Energy Convers. Manage.* **2015**, *89*, 309−317.

(2) Meier, W.; Weigand, P.; Duan, X. R.; Giezendanner-Thoben, R. Detailed characterization of the dynamics of thermoacoustic pulsations in a lean premixed swirl flame. *Combust. Flame* **2007**, *150*, 2−26.

(3) Kitano, T.; Tsuji, T.; Kurose, R.; Komori, S. Effect of Pressure Oscillations on Flashback Characteristics in a Turbulent Channel Flow. *Energy Fuels* **2015**, *29*, 6815−6822.

(4) Stöhr, M.; Boxx, I.; Carter, C.; Meier, W. Dynamics of lean blowout of a swirl-stabilized flame in a gas turbine model combustor. *Proc. Combust. Inst.* **2011**, *33*, 2953−2960.

(5) García-Armingol, T.; Ballester, J. Operational issues in premixed combustion of hydrogen-enriched and syngas fuels. *Int. J. Hydrogen Energy* **2015**, *40*, 1229−1243.

(6) Poinsot, T. Prediction and control of combustion instabilities in real engines. *Proc. Combust. Inst.* **2017**, *36*, 1−28.

(7) Ducruix, S.; Durox, D.; Candel, S. Theoretical and experimental determinations of the transfer function of a laminar premixed flame. *Proc. Combust. Inst.* **2000**, *28*, 765−773.

(8) Dowling, A. P. A kinematic model of a ducted flame. *J. Fluid Mech.* **1999**, *394*, 51−72.

(9) Schadow, K. C.; Gutmark. Combustion Instability Related to Vortex shedding in dump Combustor and their Passive control. *Prog. Energy Combust. Sci.* **1992**, *18*, 117−132.

(10) Venkataraman, K. K.; Preston, L. H.; et al. Mechanism of Combustion Instability in a Lean Premixed Dump Combustor. *J. Propul. Power* **1999**, *15*, 909−918.

(11) Tachibana, S.; Kanai, K.; Yoshida, S.; Suzuki, K.; Sato, T. Combined effect of spatial and temporal variations of equivalence ratio on combustion instability in a low-swirl combustor. *Proc. Combust. Inst.* **2015**, *35*, 3299−3308.

(12) Polifke, W.; Paschereit, C. O.; Dobbeling, K. Constructive and Destructive Interference of Acoustic and Entropy Waves in a Premixed Combustor with a Choked Exit. *Int. J. Acoust. Vib.* **2001**, *6*, 135−146.

(13) Halter, F.; Chauveau, C.; Goekalp, I. Characterization of the effects of hydrogen addition in premixed methane/air flames. *Int. J. Hydrogen Energy* **2007**, *32*, 2585−2592.

(14) Boushaki, T.; Dhue, Y.; Selle, L.; Ferret, B.; Poinsot, T. Effects of hydrogen and steam addition on laminar burning velocity of methane-air premixed flame: Experimental and numerical analysis. *Int. J. Hydrogen Energy* **2012**, *37*, 9412−9422.

(15) Syred, N.; Giles, A.; Lewis, J.; Abdulsada, M.; Medina, A. V.; Marsh, R.; Bowen, P. J.; Griffiths, A. J. Effect of inlet and outlet configurations on blow-off and flashback with premixed combustion for methane and a high hydrogen content fuel in a generic swirl burner. *Appl. Energy* **2014**, *116*, 288−296.

(16) Shoshin, Y.; Bastiaans, R. J. M.; de Goey, L. P. H. Anomalous blow-off behavior of laminar inverted flames of ultra-lean hydrogen-methane-air mixtures. *Combust. Flame* **2013**, *160*, 565−576.

(17) Hong, S.; Speth, R. L.; Shanbhogue, S. J.; Ghoniem, A. F. Examining flow-flame interaction and the characteristic stretch rate in vortex-driven combustion dynamics using PIV and numerical simulation. *Combust. Flame* **2013**, *160*, 1381−1397.

(18) Lee, J.; Jeon, S.; Kim, Y. Multi-environment probability density function approach for turbulent CH4/H-2 flames under the MILD combustion condition. *Combust. Flame* **2015**, *162*, 1464−1476.

(19) Di Sarli, V.; Di Benedetto, A.; Long, E. J.; Hargrave, G. K. Time-Resolved Particle Image Velocimetry of dynamic interactions between hydrogen-enriched methane/air premixed flames and toroidal vortex structures. *Int. J. Hydrogen Energy* **2012**, *37*, 16201−16213.

(20) Schefer, R. W. Hydrogen enrichment for improved lean flame stability. *Int. J. Hydrogen Energy* **2003**, *28*, 1131−1141.

(21) Yilmaz, I.; Ratner, A.; Ilbas, M.; Huang, Y. Experimental investigation of thermoacoustic coupling using blended hydrogen-methane fuels in a low swirl burner. *Int. J. Hydrogen Energy* **2010**, *35*, 329−336.

(22) Kim, H. S.; Arghode, V. K.; Gupta, A. K. Flame characteristics of hydrogen-enriched methane-air premixed swirling flames. *Int. J. Hydrogen Energy* **2009**, *34*, 1063−1073.

(23) García-Armingol, T.; Ballester, J. Operational issues in premixed combustion of hydrogen-enriched and syngas fuels. *Int. J. Hydrogen Energy* **2015**, *40*, 1229−1243.

(24) Shanbhogue, S. J.; Sanusi, Y. S.; Taamallah, S.; et al. Flame macrostructures, combustion instability and extinction strain scaling in swirl-stabilized premixed CH4/H2 combustion. *Combust. Flame* **2016**, *163*, 494−507.

(25) Barbosa, S.; Garcia, M. D. L. C.; Ducruix, S.; et al. Control of combustion instabilities by local injection of hydrogen. *Proc. Combust. Inst.* **2007**, *31*, 3207−3214.

(26) Emadi, M.; Kaufman, K.; Burkhalter, M. W.; et al. Examination of thermo-acoustic instability in a low swirl burner. *Int. J. Hydrogen Energy* **2015**, *40*, 13594−13603.

(27) Emadi, M.; Karkow, D.; Melendez, A.; et al. Parameter variations and the effects of hydrogen: An experimental investigation in a lean premixed low swirl combustor. *Int. J. Hydrogen Energy* **2013**, *38*, 5401−5409.

(28) Wang, M.; Zhong, Y.; Deng, K. Experiment investigation of the effects of hydrogen content on the combustion instability of methane/hydrogen lean premixed swirl flames under different acoustic frequency ranges. *AIP Adv.* **2019**, *9*, No. 045206.

(29) Balachandran, R.; Ayoola, B. O.; Kaminski, C. F.; Dowling, A. P.; Mastorakos, E. Experimental investigation of the nonlinear response of turbulent premixed flames to imposed inlet velocity oscillations. *Combust. Flame* **2005**, *143*, 37−55.

(30) Hong, S.; Shanbhogue, S. J.; Speth, R. L.; Ghoniem, A. F. On the phase between pressure and heat release fluctuations for propane/hydrogen flames and its role in mode transitions. *Combust. Flame* **2013**, *160*, 2827−2842.

(31) Hardalupas, Y.; Panoutsos, C. S.; Taylor, A. M. K. P. Spatial resolution of a chemiluminescence sensor for local heat-release rate and equivalence ratio measurements in a model gas turbine combustor. *Exp. Fluids* **2010**, *49*, 883−909.

(32) Ruggles, A.; Kelman, J. Unsteady vortex breakdown in an atmospheric swirl stabilised combustor. Part 1: Chamber behaviour. *Combust. Flame* **2015**, *162*, 388−407.

(33) Dasch, C. J. One-dimensional tomography- A comparison of Abel, Onion-peeling, and filtered backprojection metnods. *Appl. Opt.* **1992**, *31*, 1146−1152.

(34) Palies, P.; Durox, D.; Schuller, T.; et al. Nonlinear combustion instability analysis based on the flame describing function applied to turbulent premixed swirling flames. *Combust. Flame* **2011**, *158*, 1980−1991.

(35) Yu, G.; Law, C. K.; Wu, C. K. Laminar flame speeds of hydrocarbon + air mixtures with hydrogen addition. *Combust. Flame* **1986**, *63*, 339−347.

(36) Lacoste, D. A.; Xiong, Y.; Moeck, J. P.; Chung, S. H.; Roberts, W. L.; Cha, M. S. Transfer functions of laminar premixed flames subjected

https://dx.doi.org/10.1021/acsomega.0c00287
ACS Omega XXXX, XXX, XXX−XXX

to forcing by acoustic waves, AC electric fields, and non-thermal plasma discharges. *Proc. Combust. Inst.* **2017**, *36*, 4183−4192.
(37) Yoon, J.; Joo, S.; Kim, J.; Lee, M. C.; Lee, J. G.; Yoon, Y. Effects of convection time on the high harmonic combustion instability in a partially premixed combustor. *Proc. Combust. Inst.* **2017**, *36*, 3753−3761.
(38) Cuquel, A.; Durox, D.; Schuller, T. Scaling the flame transfer function of confined premixed conical flames. *Proc. Combust. Inst.* **2013**, *34*, 1007−1014.
(39) Kim, K. T.; Hochgreb, S. Measurements of triggering and transient growth in a model lean-premixed gas turbine combustor. *Combust. Flame* **2012**, *159*, 1215−1227.
(40) Candel, S.; Durox, D.; Schuller, T.; Bourgouin, J.-F.; Moeck, J. P. Dynamics of Swirling Flames. *Annu. Rev. Fluid Mech.* **2014**, *46*, 147−173.
(41) Preetham, R.; Santosh, H.; Lieuwen, T. Dynamics of Laminar Premixed Flames Forced by Harmonic Velocity Disturbances. *J. Propul. Power* **2008**, *24*, 1390−1402.
(42) Di Sarli, V.; Di Benedetto, A. Effects of non-equidiffusion on unsteady propagation of hydrogen-enriched methane/air premixed flames. *Int. J. Hydrogen Energy* **2013**, *38*, 7510−7518.
(43) Therkelsen, P. L.; Portillo, J. E.; Littlejohn, D.; Martin, S. M.; Cheng, R. K. Self-induced unstable behaviors of CH4 and H-2/CH4 flames in a model combustor with a low-swirl injector. *Combust. Flame* **2013**, *160*, 307−321.

https://dx.doi.org/10.1021/acsomega.0c00287
ACS Omega XXXX, XXX, XXX−XXX